



Reduced Cone Density Is Associated with Multiple Sclerosis

Gemma McIlwaine, MSc,¹ Lajos Csincsik, PhD,^{1,2} Rachel Coey, BSc,¹ Luping Wang, MD, PhD,¹ Denise Fitzgerald, PhD,¹ Jill Moffat, BSc,¹ Adam M. Dubis, PhD,³ Gavin McDonnell, MD,⁴ Stella Hughes, MD,⁴ Tunde Peto, MD, PhD,² Imre Lengyel, PhD¹

Purpose: Multiple sclerosis (MS) is an inflammatory neurodegenerative disease of the central nervous system. Recent evidence suggests that degeneration of the inner layers of the retina occurs in MS. This study aimed to examine whether there are outer retinal changes in patients living with MS.

Design: This was a single center, cross-sectional study.

Participants: Sixteen patients with MS and 25 controls (volunteers without diagnosed MS) were recruited for the study.

Methods: We acquired volumetric spectral domain-OCT scans of the macula and a circular scan around the optic nerve head (ONH). We also captured adaptive optics (AO) images at 0° (centered on the foveola), 2°, 4°, and 6° temporal to the fovea.

Main Outcome Measures: We calculated the thickness of the different retinal layers in the macula and around the ONH using the inbuilt software of the OCT. We evaluated changes in cone photoreceptors by calculating cone density and spacing by the inbuilt AO automatic segmentation algorithm with manual correction. We compared patients with and without optic neuritis and controls.

Results: We found significant thinning of the inner retina and a thickening of the outer retina in the eye with a history of optic neuritis (eyes of patients with MS with a history of optic neuritis; mean difference [MD]: $-11.13 \pm 3.61 \mu\text{m}$, $P = 0.002$ and MD: $2.86 \pm 0.89 \mu\text{m}$, $P = 0.001$; respectively). We did not observe changes in retinal layers without optic neuritis in eyes of patients with MS without a history of optic neuritis. However, regional differences were detected in the peripapillary retinal nerve fiber layer. Analyzing AO images revealed a significantly lower cone outer-segment density at all eccentricities in all patients compared with control eyes ($P < 0.05$), independent of optic neuritis history.

Conclusions: Our results showed that all MS cases were associated with decreased cone densities. Future longitudinal studies will help to elucidate whether this is a specific and sensitive method to detect and monitor the development and progression of MS.

Financial Disclosure(s): Proprietary or commercial disclosure may be found after the references. *Ophthalmology Science* 2023;3:100308 © 2023 Published by Elsevier Inc. on behalf of the American Academy of Ophthalmology. This is an open access article under the CC BY-NC-ND license (<http://creativecommons.org/licenses/by-nc-nd/4.0/>).

Multiple sclerosis (MS) is an inflammatory, neurodegenerative disease of the central nervous system.¹ Up to 80% of patients with MS will experience ocular pathology during their disease course.² In the eye, MS is reported to be associated with the degeneration of the macular ganglion cell-inner plexiform layer (GCIPL) and peripapillary retinal nerve fiber layer (pRNFL).³ However, degeneration of the inner retinal layers does not fully explain the visual deterioration in MS patients.^{1,4–7} For example, the correlations between inner retinal thinning and impaired visual function are mild to moderate at best.^{2,6–8} In addition, Hanson et al⁴ did not find a relationship between inner retinal layer thickness and electroretinogram values. However, previous studies did not report outer retinal changes in MS. In the Belfast Eye and MS study, we analyzed inner and outer retinal changes using OCT and examined photoreceptor changes using adaptive optics (AO) imaging.

To our knowledge, this is the first report examining outer retinal changes, in detail, in patients with MS.

Methods

The Belfast Eye and MS study is a single centre, cross-sectional, case-control study approved by the United Kingdom research ethics committee (REC 18/NW/0334). All participants gave written consent. Patients with MS (N = 16) were recruited from the Northern Irish MS Research Network cohort. All MS patients were stratified by consultant neurologists (G.McD. and S.H.) based on the revised McDonald criteria, 2010.⁹ Control participants (N = 25) were recruited from the Queen's University, Belfast community, including staff and students. Participant demographics, including disease status, optic neuritis history, treatment/medications, Expanded Disability Scale Score, and other comorbidities, including the use of hypertensive medication and diabetes, were obtained from medical records. For the

control participants, this information was collected by using a health questionnaire. Patients with a history of optic neuritis ≤ 6 months before the study visit were excluded. No patients had optic neuritis at the time of study visit.

Spherical error (Shin Nippon Accuref K-900), intraocular pressure (IOP; Reichert Ocular Response Analyzer), visual acuity (VA) (ETDRS Charts) and contrast sensitivity (Pelli Robson Contrast Sensitivity charts) were measured before the pupils were dilated using 1% w/v Tropicamide. After dilation, OCT scans by Spectralis OCT2 (Heidelberg Engineering) and AO images by rtx1 camera (Imagine-Eyes) were acquired to assess changes in retinal thickness and cone outer-segment density and spacing, respectively.

For OCT, fovea-centered posterior pole scans and optic nerve head (ONH)-centered circular scans were acquired using Automatic Real-Time Tracking in Nsite mode. The posterior pole scans comprised 61 vertical B scans; each averaged 15 times (768 A-scans/B-scan), spaced 120 μm apart, with a total scanned area size of 30×25 . The 3.4 mm diameter ONH scan consisted of 30 averaged circular B-scans.

Retinal layers were automatically segmented using the Heidelberg Eye Explorer (Heyex) software (version 6.16.6.0). Segmentation errors were manually corrected by a trained grader (G.M.), masked to the participants' disease status. To assess neurodegeneration, thickness values of pRNFL for each sector of the ONH-centered grid and the global average pRNFL thickness were extracted alongside papillomacular bundle thickness and nasal to temporal ratio of the pRNFL thickness. Global GC IPL (inner boundary of ganglion cell to outer boundary of inner plexiform layer), whole retina (inner limiting membrane to Bruch's membrane [BM]), inner retina (inner limiting membrane to outer boundary of the outer nuclear layer), and outer retina (outer boundary of the outer nuclear layer to BM) thickness from posterior pole scans were also extracted as an average value of the foveal-centered ETDRS grid sectors.

Outer retinal changes were assessed on posterior pole scans by extracting the outer nuclear layer (ONL), retinal pigment epithelium layer, and photoreceptor segments layer (PRL; inner boundary of photoreceptor innersegment to the outer boundary of photoreceptor outersegment) thickness as an average value of the foveal-centered ETDRS grid sectors. All measurements agree with the nomenclature advised by the APOSTEL 2.0 recommendations.¹⁰

Retinal images (4×4 with a resolution of 1.25 $\mu\text{m}/\text{pixel}$ nominally) were acquired at 0° , 2° , 4° , and 6° eccentricity using AOImage (version 3.4_SP2) and analyzed using AODetect (version 3.0_SP2). Image qualities were visually assessed in the AOImage application. For analysis, 0.21×0.21 regions of interest were identified and cones were automatically detected using the AODetect application, followed by manual adjustment by an expert grader (G.M.). In a few cases, the participants were unable to focus on the exact location of the internal target which resulted in an unknown focus location in 7 eyes from 7 participants (4 patients and 3 controls). To correct for gaze, AO images were exported into ImageJ in a *.tif format¹¹ and montaged together using the plugin "MosaicJ."¹² Then the montage was superimposed onto the confocal scanning laser ophthalmoscope (cSLO) images from the OCT using GNU Image Manipulation Programme (GIMP, The GNU Development)¹³ to identify the location of the foveal-center and the eccentricities of the images.

Overall, 72.5% of eyes had ≥ 1 image analyzed, a success rate higher than previously reported.¹⁴ The reasons for exclusion are summarized in Figure 1. This included 68.75% of all control eyes, 70% of eyes of patients with MS with a history of optic neuritis (MSON), and 81.82% of eyes of patients with MS without a history of optic neuritis (MSnON). The number of eyes that did not

produce analyzable images totaled 22. This included 15 control eyes, 3 MSON eyes, and 4 MSnON eyes: due to participant fatigue with or without severe cognitive difficulties (1 control eye, 1 MSON eye, and 1 MSnON eye); 7 eyes were due to lens opacity and/or drusen (6 control eyes and 1 MSON); 4 eyes were due to the wrong location being imaged due to inability to focus on the internal target (2 control and 2 MSnON); bug within the acquisition software (3 control, 1 MSON and 1 MSnON eyes); and lack of appropriate focus on the photoreceptors (3 control eyes, 2 due to prior Lasik surgery for high myopia).

One hundred and fifty-nine (159) regions of interest from 7 control, 5 MSON, and 5 MSnON eyes were recounted to test the intraobserver reproducibility. The grading was carried out masked to diagnosis status.

Statistical Analysis

Eyes from patients with MS were subgrouped into MSON and MSnON.

Statistical significance thresholds were set to $P > 0.05$. Patient demographics were analyzed using Kruskal-Wallis and ad hoc Bonferroni analysis for continuous variables and Pearson's Chi-squared test for categorical variables for comparison between control, MSON, and MSnON. For demographics only related to patients with MS, for example, treatment or disease duration, a Mann-Whitney U Test was used to compare MSON and MSnON.

OCT and functional eye test data were analyzed using a Generalized Estimating Equitation (GEE) (exchangeable working correlation matrix) with age, gender, IOP, hypertension, and spherical error as covariates (Table 1). The use of GEE allowed controlling for the possibility of data clustering due to both eyes from 1 individual being included in the OCT analysis. The pRNFL sector thicknesses are not entirely independent and so the Bonferroni correction was applied to the GEE model. Multiple non-parametric Mann-Whitney U tests with ad-hoc Hölm-Šidák test were used to compare photoreceptor density between control and MS groups at each eccentricity. A 2-way (parametric) analysis of variance and ad-hoc Tukey's test were used to compare photoreceptor density between control, MSON, and MSnON groups at each eccentricity. For reproducibility analysis of cone density, an intraclass correlation coefficient was used (Fig 5D). Bland-Altman analysis was also used to determine the "bias" (the mean difference [MD] between 2 methods of measurement) and 95% limits of agreement.

Results

Participant Demographics

Of the 41 participants recruited (25 controls and 16 patients with MS), 40 were included in the final analysis. One control participant was excluded from the analysis due to a family history of MS and ongoing neurological symptoms that required further investigation to exclude MS. Thirteen patients were diagnosed with relapsing-remitting MS, and 3 patients were diagnosed with secondary progressive MS. Eleven patients with MS were on disease-modifying therapy (7 on natalizumab, 2 on interferon-beta treatment, 1 on glatiramer acetate, and 1 on dimethyl fumarate). Five patients were not receiving any disease-modifying therapy for MS (nontreated). No significant differences were found in age between patients with MS (50.81 ± 2.65 years) and controls (48.33 ± 2.30 years) or gender distribution ($P = 0.292$).

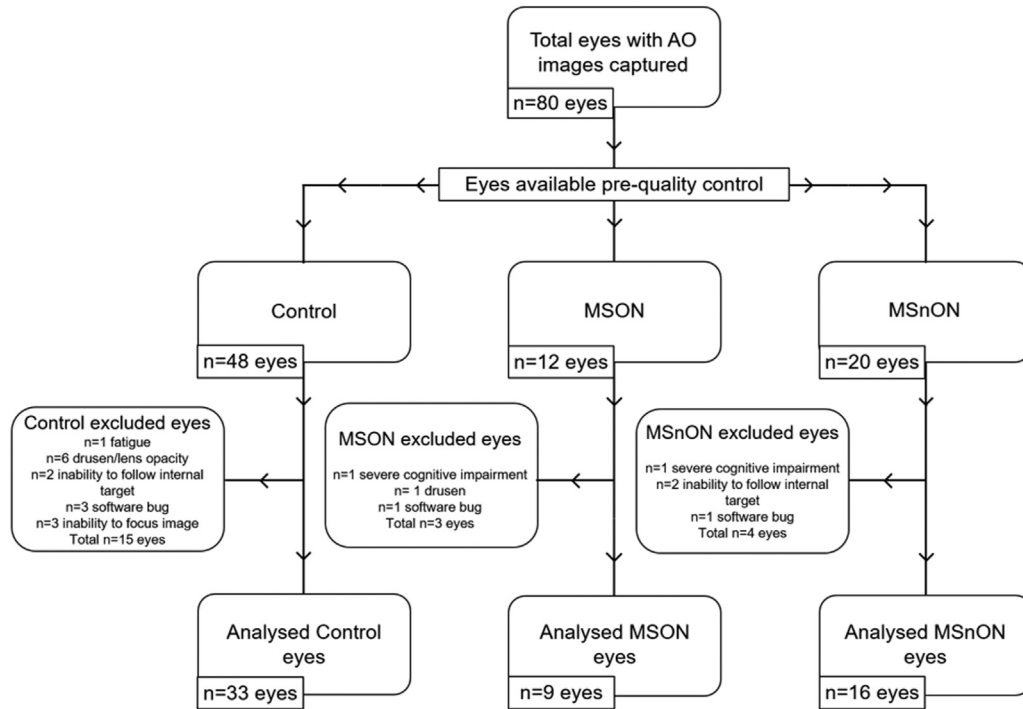


Figure 1. Flow chart of analyzed adaptive optics (AO) images from control, eyes of patients with MS with a history of optic neuritis (MSON), and eyes of patients with MS without a history of optic neuritis (MSnON) participants.

Of the 32 eyes from the 16 patients with MS, 12 had a known history of optic neuritis (MSON), and 20 did not (MSnON). No optic neuritis was reported in the control group. No significant differences were found in age between patients with MSON (55.50 ± 3.13 years) and MSnON (48.00 ± 2.10 years), and there were no differences in gender distribution ($P = 0.292$). No significant differences in Expanded Disability Scale Score were found between MSON (3.80 ± 1.08) and MSnON (3.44 ± 0.57), $P = 0.134$, or in disease duration between MSON (23.40 ± 6.76) and MSnON (15.91 ± 3.19), $P = 0.148$.

There was a significant difference in the proportion of patients on antihypertension medication between the 3 groups (Chi-square, $P = 0.015$). Four (8.3%) control eyes, 5 (41.7%) MSON eyes, and 5 (25%) MSnON eyes were from participants prescribed antihypertension medication. Eyes within the MSON (13.10 ± 0.86) and MSnON (12.96 ± 0.41) groups had significantly lower IOP compared with controls (15.82 ± 0.78) ($P = 0.031$ and $P = 0.012$, respectively). Therefore, hypertension and IOP were among the covariates incorporated into the GEE analysis. All covariates included in the GEE analysis are summarized in Table 1. No significant differences were found between MSON and MSnON in Expanded Disability Scale Score or disease duration ($P = 0.134$ and $P = 0.148$, respectively).

OCT Segmentation

After segmentation of the circular ONH scans, we found a significant thinning of the global pRNFL (Fig 2A) in MSON

compared with the control (MD was $-20.52 \pm 5.89 \mu\text{m}$, $P < 0.001$). No difference was observed between MSnON and controls ($P = 1.0$). The papillomacular bundle (the fibers that run directly from the optic nerve to the fovea) was thinned in both MSON (MD: $-16.96 \pm 4.12 \mu\text{m}$, $P < 0.001$) and MSnON (MD: $-6.87 \pm 2.69 \mu\text{m}$, $P = 0.021$) compared with controls (Fig 2B). The nasal-to-temporal ratio of the rPNFL thickness was significantly increased between controls and MSON (MD: 0.37 ± 0.10 , $P < 0.001$) but not between controls and MSnON (MD: 0.19 ± 0.10 , $P = 0.09$) (Fig 2C). A significant thinning was seen between MSON and controls in the temporal sector (MD: $-22.70 \pm 5.45 \mu\text{m}$, $P < 0.001$) but no significant difference was seen in MSnON compared with controls (MD: -5.85 ± 3.17 , $P = 0.169$) (Fig 2D). A significant thinning was observed in MSON compared with controls in temporal-superior (MD: $-25.90 \pm 6.22 \mu\text{m}$, $P < 0.001$) (Fig 2E) and temporal-inferior (MD: $-33.89 \pm 10.22 \mu\text{m}$, $P = 0.002$) (Fig 2F) sectors but no significant thinning was seen in these sectors between MSnON and controls ($P > 0.05$). No significant difference was seen for the nasal pRNFL between controls and MSON or MSnON (Fig 2G). When the nasal-superior sector was segmented we found a significant thinning between controls and both MSON (MD: $-21.76 \pm 9.61 \mu\text{m}$, $P = 0.047$) and MSnON (MD: $-22.75 \pm 5.48 \mu\text{m}$, $P < 0.001$) compared with controls (Fig 2H), while there was no difference when the superior nasal sectors were compared (Fig 2I). The findings were summarized graphically for MSON (Fig 2J) and MSnON (Fig 2H) where significant differences are highlighted by red.

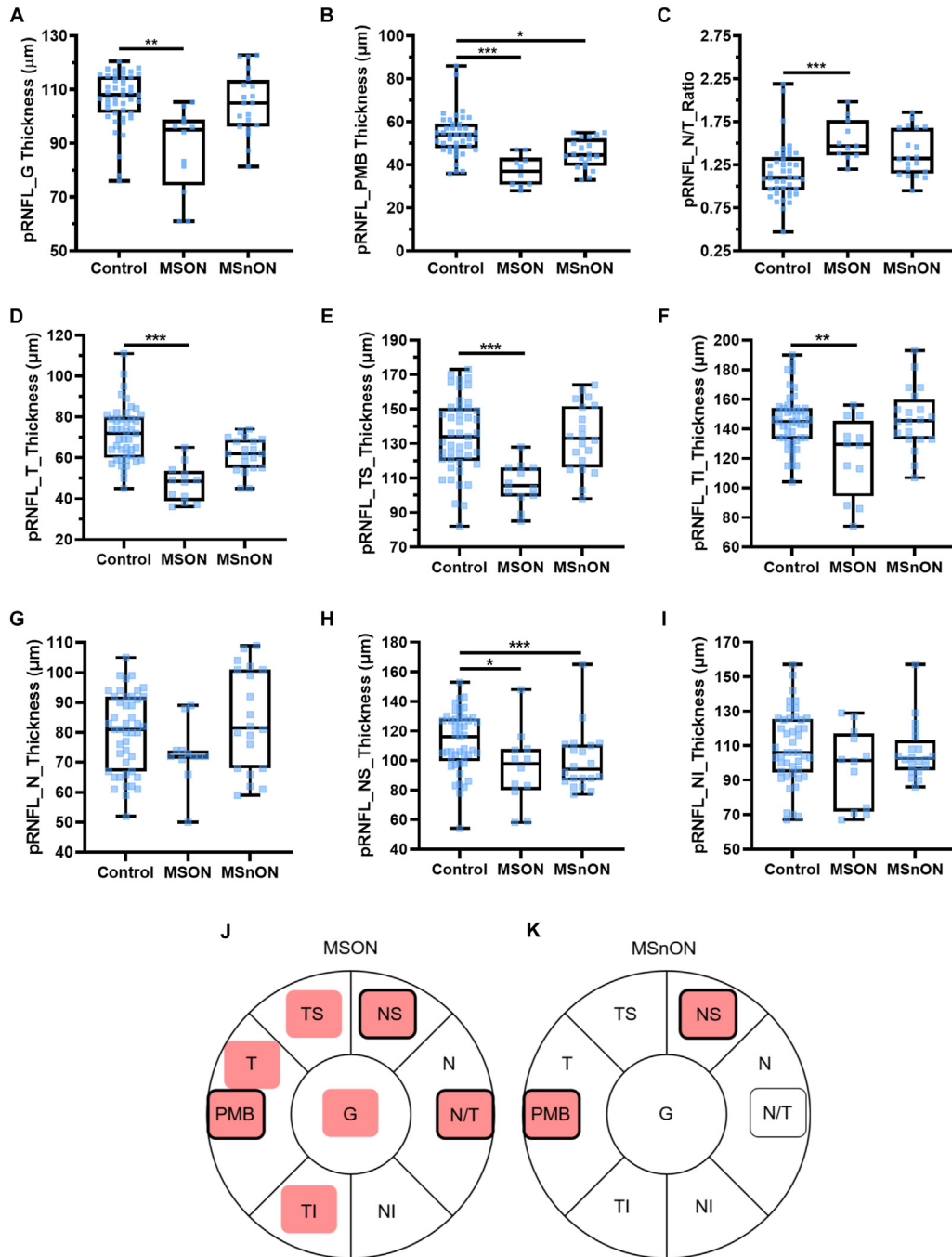


Figure 2. Analysis of the peripapillary retinal nerve fiber layer (pRNFL) on OCT images (Control, n = 41–42, eyes of patients with MS with a history of optic neuritis [MSON], n = 11–12; eyes of patients with MS without a history of optic neuritis [MSnON], n = 18 eyes): (A) global [G]; (B) papillomacular bundle [PMB]; (C) nasal to temporal ratio [N/T]; (D) temporal [T] sector; (E) temporal-superior [TS] sector; (F) temporal-inferior [TI]; (G) nasal [N] sector; (H) nasal-superior [NS]; (I) nasal-inferior [NI] sector; J and K are graphical representations of results from A–I for all sectors around the optic nerve. The pink background represents significant thinning; those that change in MSON and MSnON are outlined in black. All box and whisker plots represent the 25th–75th percentile with a line at the median (50th percentile). Whiskers represent the range of the data. Each data point represents one eye. * < 0.05; ** < 0.01; *** < 0.001.

When the thickness of the whole retina (inner limiting membrane to BM) was compared, no significant differences were observed between the control and MSON ($P = 0.24$) or MSnON ($P = 0.738$) (Fig 3A). Assessing the posterior pole scans, we found a trend toward a significant

difference in the inner retina (RNFL–ONL) in MSON compared with controls (MD: -12.48 ± 7.10 $P = 0.08$). Still, no difference was found in MSnON compared with controls ($P = 0.768$) (Fig 3B). The thickness of the combined GCIPL layers was thinned in MSON

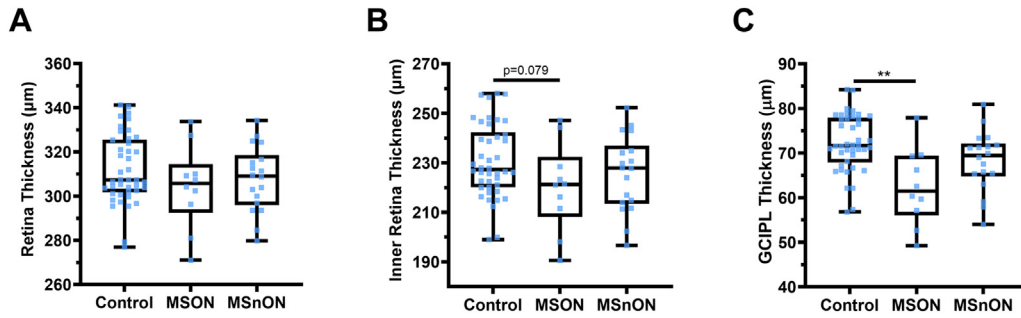


Figure 3. No significant differences were measured in whole retina thickness (A) and the combined inner retinal layer thicknesses (B). However, there was a significant decrease in ganglion cell inner plexiform layer (GCIPL) in eyes of patients with MS with a history of optic neuritis (MSON) compared with controls (C). Control n = 42, MSON n = 10, eyes of patients with MS without a history of optic neuritis (MSnON) n = 18. Each data point represents one eye. * < 0.05; ** < 0.01; *** < 0.001.

(MD: $-11.33 \pm 3.90 \mu\text{m}$, $P = 0.004$) but not in MSnON ($P = 0.57$) (Fig 3C). The cell bodies of the photoreceptor cells reside within the ONL. There was no significant difference in the thickness of the ONL between controls and MSON ($P = 0.59$) or MSnON ($P = 0.47$) (Fig 4A).

However, there was a significant difference in the thickness of the combined photoreceptor inner and outer segments (PRL) in MSON compared with control (MD: $3.43 \pm 0.75 \mu\text{m}$ $P < 0.001$) but no significant difference was observed between control and MSnON ($P = 0.11$)

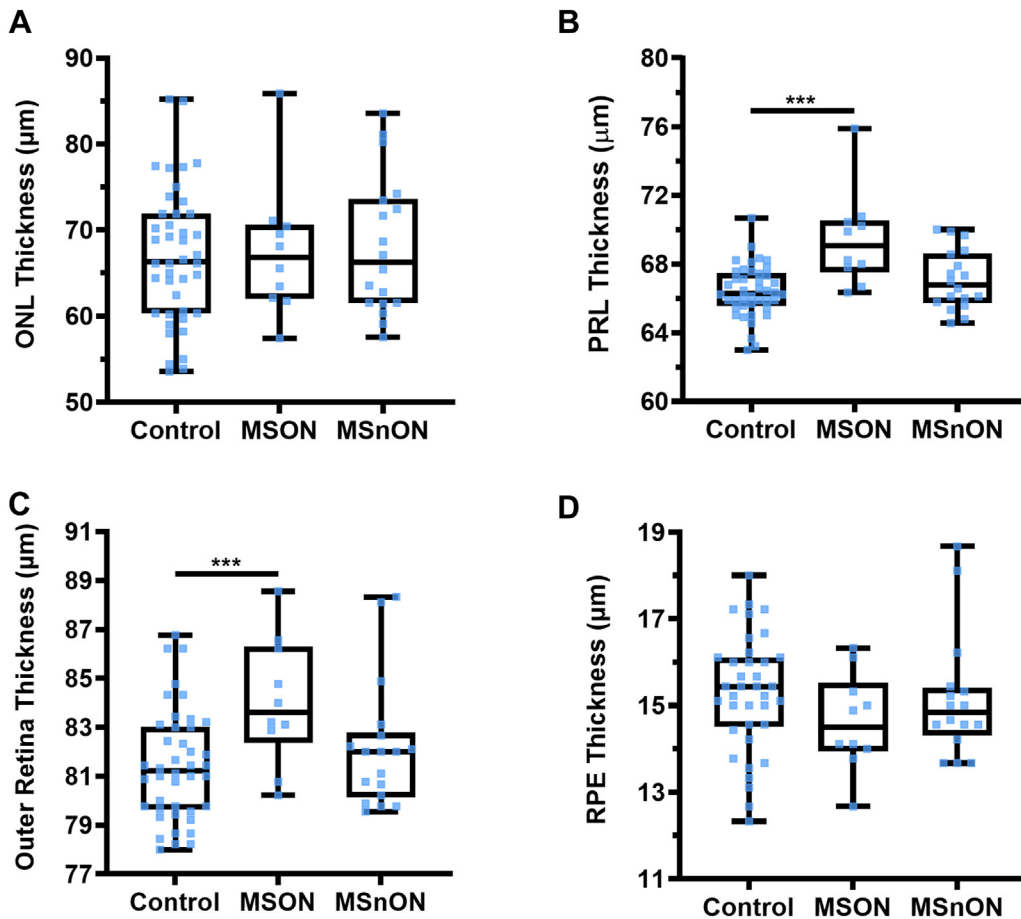


Figure 4. Analysis of the outer retinal layers on OCT images (Control, n = 42, eyes of patients with MS with a history of optic neuritis [MSON], n = 12; eyes of patients with MS without a history of optic neuritis [MSnON], n = 18 eyes): (A) outer nuclear layer (ONL); (B) photoreceptor layer (PRL); (C) combined outer retinal layers; (D) retinal pigment epithelium (RPE) layer. All box and whisker plots represent the 25th–75th percentile with a line at the median (50th percentile). Whiskers represent the range of the data. Control n = 42, MSON n = 10, MSnON n = 18. Each data point represents 1 eye. * < 0.05; ** < 0.01; *** < 0.001.

Table 1. Participant Demographics

| Demographic | Control | MSON | MSnON | Statistical Comparison |
|---|------------------|------------------|------------------|---------------------------------|
| Number of eyes | 48 | 12 | 22 | - |
| Age (years) | | | | |
| Range | 28–71 | 44–73 | 43–65 | Overall $P = 0.155^*$ |
| Mean \pm SEM | 48.33 \pm 1.64 | 55.50 \pm 3.13 | 48.00 \pm 2.10 | Control vs. MSON $P = 0.214^*$ |
| | | | | Control vs. MSnON $P = 1.0^*$ |
| | | | | MSON vs. MSnON $P = 0.234^*$ |
| Gender (% female) | 32 (66.7) | 7 (70) | 9 (40.9) | $P = 0.098^\dagger$ |
| Spherical error equivalent (Diopters) | -0.26 \pm 0.26 | 1.87 \pm 0.88 | 0.61 \pm 0.24 | Overall $P = 0.051^*$ |
| | | | | Control vs. MSON $P = 0.077^*$ |
| | | | | Control vs. MSnON $P = 0.404^*$ |
| | | | | MSON vs. MSnON $P = 1.0^*$ |
| Hypertension medication n (%) | 4 (8.3) | 5 (41.7) | 5 (25) | $P = 0.015^\ddagger$ |
| Intraocular pressure (IOP) mean \pm SEM | 15.82 \pm 0.78 | 13.10 \pm 0.86 | 12.96 \pm 0.41 | Overall $P = 0.002^*$ |
| | | | | Control vs. MSON $P = 0.031^*$ |
| | | | | Control vs. MSnON $P = 0.012^*$ |
| | | | | MSON vs. MSnON $P = 1.0^*$ |

IOP = intraocular pressure; MSON = eyes with a history of optic neuritis (from patients with multiple sclerosis); MSnON = eyes without a history of optic neuritis (from patients with multiple sclerosis); SEM = standard error of the mean.

Hypertension medication given as number of eyes from a participant prescribed hypertension medication at time of study visit.

All demographics presented were used as covariates in the Generalized Estimating Equitation model for OCT analysis.

‡ Mann-Whitney U-test.

$*$ Kruskall-Wallis ad hoc Bonferroni.

† Chi-square.

(Fig 4B). The outer retinal layers (external limiting membrane to BM) were significantly increased in MSON compared with controls (MD: 2.86 \pm 0.89 μ m, $P = 0.001$) but not MSnON compared with controls ($P = 0.573$) (Fig 4C). There was no significant difference in the thickness of the retinal pigment epithelium layer between controls and MSON ($P = 0.89$) or MSnON ($P = 0.53$) (Fig 4D).

Analysis of Cone Densities on AO Images

To better understand the changes associated with PRL in MS, we imaged all eyes with AO at 0–8 degrees eccentricity temporal to the foveola. We found that cone outer-segment density was significantly lower in patients with MS compared with controls at all eccentricities; 2° $P = 0.005$, 2.5° $P = 0.001$, 3° $P = 0.001$, 3.5° $P = 0.021$, 4.5° $P = 0.005$, 5.5° $P = 0.005$ and 7° $P = 0.035$) (Fig 5A). An increase in spacing between cone outer segments accompanied the decreased cone density at all eccentricities (2.0° $P < 0.001$, 2.5° $P < 0.001$, 3.0° $P < 0.001$, 3.5° $P < 0.001$, 4.5° $P < 0.001$, 5.5° $P < 0.001$, 7.0° $P < 0.001$; multiple Mann-Whitney tests, ad-hoc Tukey's) (Fig 5B). The decrease in cone densities ranged between 13.10% and 5.32% in all MS (Fig 5C). Intragrader reliability was high as the intraclass correlation coefficient was 0.971 (Fig 5D), and the Bland-Altman bias was 318 cones/mm² (standard deviation \pm 1593 and 95% limits of agreement between -2805 and 3441 cones/mm²; Fig 5E).

Due to the thinning of layers within the inner retina between controls and MSON, we investigated the effect of optic neuritis history on the cone density. We found a significant decrease in the cone density compared with controls in both MSON ($P < 0.001$ at all eccentricities) and MSnON

($P < 0.001$ at all eccentricities) (Fig 6A). There was no significant difference between MSON and MSnON ($P > 0.99$). We also found an increase in cone spacing compared with controls in MSON and MSnON ($P < 0.001$ at all eccentricities). There were no significant differences between MSON and MSnON ($P > 0.873$ at all eccentricities) (Fig 6B).

Functional Vision Tests

Multiple sclerosis has been associated with decreased VA.^{2,15} Therefore, we tested VA for all participants and all eyes (Fig 7). We found a trend for worsening VA in MSON compared with controls (MD: 0.13 \pm 0.07, $P = 0.080$) but no significant difference was detected between controls and MSnON ($P = 0.962$). Contrast sensitivity was lower in eyes with MSON than in controls (MD: -0.15 \pm 0.05, $P < 0.005$), but no significant difference was found between controls and eyes with MSnON ($P = 0.216$).

Discussion

In this study, we reproduced the previously reported inner retinal thinning in MS^{7,16,17} in those with a history of optic neuritis (MSON). In addition, for the first time, we report significantly lower cone density independent of optic neuritis and a thickening of the combined PRL in MSON eyes.

Some degree of ocular inflammation is common in those diagnosed with MS,^{18,19} with approximately 50% of patients with MS experiencing optic neuritis.^{20,21} Longitudinal studies have reported that inner retina thinning occurs in both MSON and MSnON.^{1,4,5,20} However, in our cross-sectional study only MSON

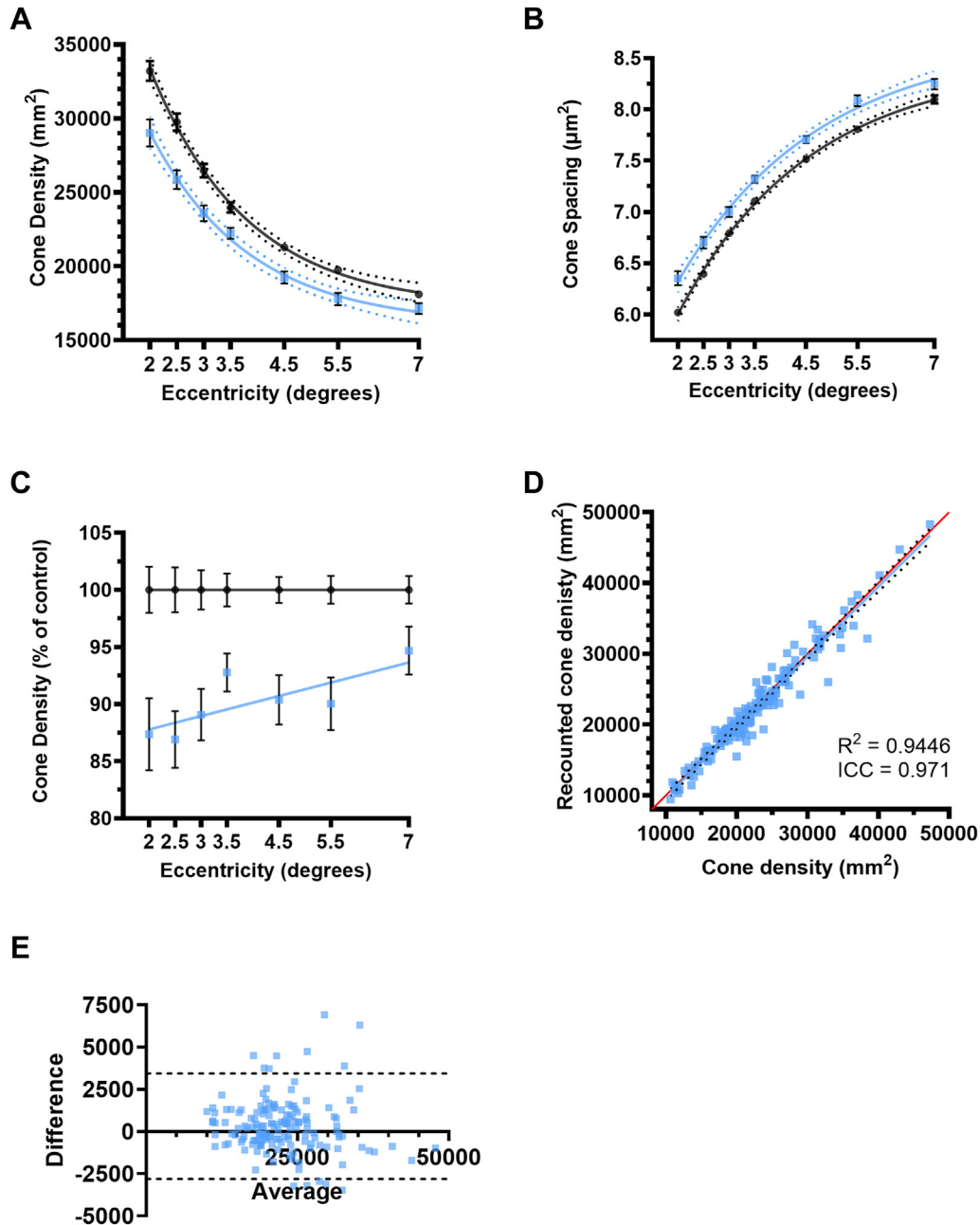


Figure 5. Analysis of the results from the adaptive optics imaging (A) cone density; (B) cone spacing; (C) cone density normalized to controls; (D) recounted cone density to determine intra-grader reproducibility, red line represents $x = y$ and dotted line represents 95% confidence intervals. The black circles are the averages of cone densities from controls at different eccentricities and the blue squares are the averages from patients with multiple sclerosis (MS) on A–C, error bars represent standard error of the mean and dotted lines represent 95% confidence intervals (E) Bland-Altman plot showing reproducibility bias and 95% limits of agreement (black dotted lines), Control, $n = 22$ –32, eyes of patients with MS with a history of optic neuritis, $n = 6$ –8; eyes of patients with MS without a history of optic neuritis $n = 11$ –14 eyes. ICC = intraclass correlation coefficient.

showed significant thinning of the global average pRNFL (Fig 2A) and GCIPL (Fig 3C). Therefore, in order to understand the natural history and provide better prognostication to our patients, detailed monitoring of the retinal layers in follow-up studies will be necessary.

Both our and Birkeldh’s data support that there are likely to be regional differences in pRNFL thickness, with some

regions, such as the papillomacular bundle and nasal-superior sectors, showing thinning even in those with MSnON.²² In contrast, other sectors might be spared.²²

Despite the significant differences in the inner retinal layers, the groups did not differ in whole retina thickness (RNFL-BM) in the macula (Fig 3A). Our hypothesis was, therefore, that this might be due to an increase in outer

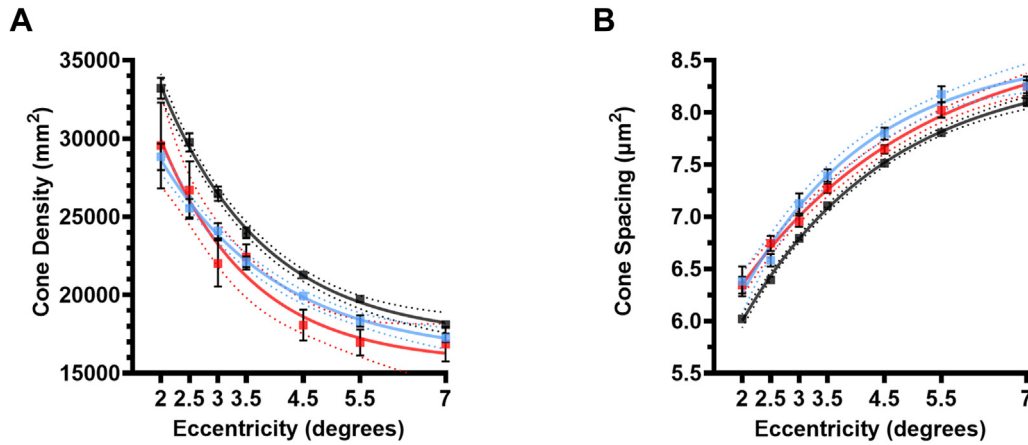


Figure 6. Comparison of cone densities (A) and spacing (B): (A) cone density (G); (B) cone spacing. The black circles are the averages of cone densities from Controls at different eccentricities, the blue squares are the averages from eyes of patients with multiple sclerosis (MS) without a history of optic neuritis (MSnON) and the red circle are the averages eyes of patients with MS with a history of optic neuritis with (MSON). Control n = 20–32, MSON, n = 8–10; MSnON, n = 9–12 eyes.

retinal layers' thickness. In our patients with MSON, there was a thickening in the outer retina and PRL (Fig 4B, C). No such finding was present in a previous study, but this is likely due to the differences in measurement boundaries, as Sabaner et al²³ measured the combined PRL + retinal pigment epithelium and did not report on PRL-only measurements. Fard et al²⁴ found a thickening of ONL due to acute optic neuritis, a finding we could not replicate as our study excluded those with ongoing or recent (< 6 months) optic neuritis. Therefore, the patient populations are not directly comparable. We propose that the observed PRL thickening in our nonacute cohort was not due to acute inflammation caused by optic neuritis but may be linked with chronic inflammation in the photoreceptor layer. In our well-characterized patient cohort, we found an approximately 15% lower cone photoreceptor density and increased spacing between cones

on AO images (Fig 4A, B). Due to our study's cross-sectional nature, we cannot determine causality, nor can we identify which stage of the disease this might have started. There is no comparable data on MS published so far. Still, based on a recent report in patients with rod-cone dystrophy (a genetic disease known to cause photoreceptor cell death) reporting an 11% reduction in cone density being pathological,²⁵ our findings of 15% loss in MS is likely to be physiologically significant. Adaptive optics imaging has not previously been used to study retinal changes in patients with MS, but the noninvasive and reproducible nature of such imaging methods and our discriminative results of loss of photoreceptors suggest photoreceptor density and spacing as imaged by AO might become a valuable tool in the future.

In our study, lower cone densities were present in MSON and MSnON patients, while changes in inner layer

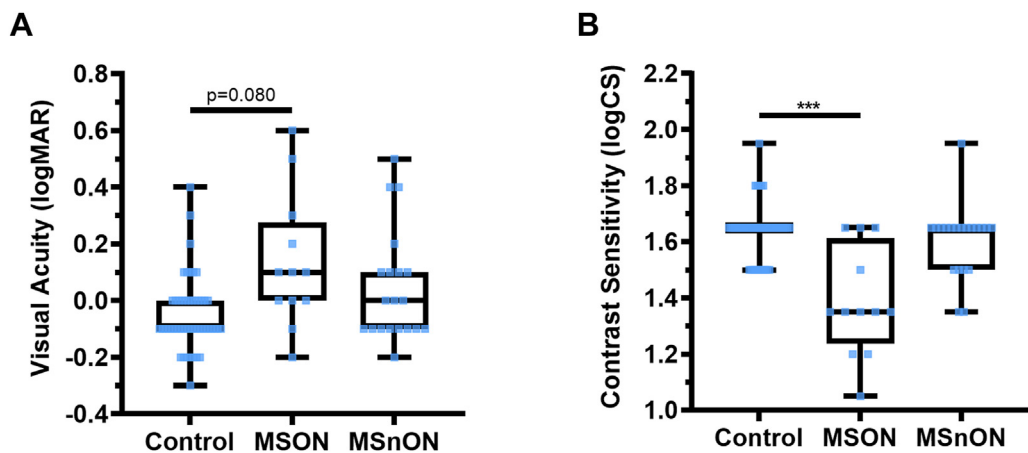


Figure 7. Visual acuity (logMAR; A) and contrast sensitivity (logCS; B) show that controls perform better in functional vision tests than patients with multiple sclerosis (MS) with a history of optic neuritis (MSON), though no significant differences were found between controls and patients with MS without a history of optic neuritis (MSnON). Each data point represents a measurement from 1 eye. Control n = 48, MSON n = 12 and MSnON n = 20 eyes. Box and whisker plots- boxes represent the 25th and 75th percentile with a line at the median (50th percentile). Whiskers represent the range of data. * < 0.05; ** < 0.01; *** < 0.001. logMAR = logarithm of the minimum angle of resolution.

thicknesses on OCT appear to have only reached significance in MSON. Therefore, AO imaging might be a sensitive and possibly a more specific indicator of retinal changes in MS than OCT imaging, or the 2 together might contribute to a more detailed phenotyping of MS patients. Our AO equipment did not allow for the imaging of rod densities. Previous evidence suggests that rods are more susceptible to inflammatory insults than cones.²⁶ Therefore, rod densities might also decrease in MS, and so once available, imaging and analysis of relevant parameters for the rods will need to be established.

Functional changes might not always accompany morphological changes in the retina. In our cohort, a reduced contrast sensitivity was measured only in patients with MSON, a finding that paralleled previous results.¹⁵ Contrast sensitivity, as measured, is unlikely to be sensitive enough to show functional changes associated with the approximately 15% photoreceptor deficit seen in our cohort.² While we had no access to carrying out electroretinograms, these are sensitive to retinal dysfunction and identification of cell-specific responses with outer retinal dysfunction having been previously shown in MS.³ Bringing together sensitive morphological and functional testing in the future will help to elucidate what battery of tests might be best to monitor the development and progression of MS.

The strength of our study is that our patients are well-characterized and have been under the care of a specific research-active clinical team. The battery of tests was carried out by trained and certified operators, and the detailed analysis of the imaging was done under strict reading center

conditions. Northern Ireland has 1 of the highest prevalences of MS worldwide, and therefore we believe that misdiagnosis was unlikely in our cohort.

We acknowledge that our study has limitations. Our sample size was small and predominantly White and, therefore, may not fully represent the MS population around the world. Using both eyes from all individuals may promote the clustering of data. However, modeling our data using GEE allowed us to correct for clustering. As we had no opportunity to measure axial length, to overcome this limitation, we integrated spherical error into our statistical models, which has previously been shown to have a good correlation with axial length.²⁷

Conclusion

In conclusion, this is the first study to show lower photoreceptor outer densities and spacing in patients with MS, suggesting that AO retinal imaging has the potential to become a sensitive marker for MS. Whether the observed changes in this cross-sectional study can be translated to a larger and more ethnically diverse population remains to be seen.

Acknowledgments

The authors thank the participants and their careers for taking part in this study. The authors would also like to thank Northern Ireland Clinical Research Facility team members for their help throughout the BEAMS study. We also thank OPTOS PLC for the unrestricted grant that supported the study, including the PhD studentship for G.M.

Footnotes and Disclosures

Originally received: February 13, 2023.

Final revision: April 1, 2023.

Accepted: April 6, 2023.

Available online: April 13, 2023. Manuscript no. XOPS-D-23-00034.

¹ Wellcome Wolfson Institute for Experimental Medicine, Queen's University Belfast, Belfast, UK.

² Centre for Public Health, Queen's University Belfast, Belfast, UK.

³ UCL Global Business School for Health, University College London, London, UK.

⁴ Department of Neurology, The Royal Victoria Hospital, Belfast Health and Social Care Trust, Belfast, UK.

Disclosures:

All authors have completed and submitted the ICMJE disclosures form.

The authors made the following disclosures: L.W., R.C., J.M., and G.McD. report no conflict of interest, A.M.D. reports personal fees from Boston Micromachines Corp, outside the submitted work; D.F. reports grants and personal fees from Sangamo Inc, outside the submitted work and Ongoing research collaboration with membership of SAB of Sangamo Inc; I.L., P.T., and G.McI. report grants from Optos Plc, during the conduct of the study; L.C. reports grants from Queen's University Belfast, during the conduct of the study; S.H., reports personal fees from Biogen, personal fees from Novartis, outside the submitted work. We report here for the first time that there is a lower cone photoreceptor density associated with multiple sclerosis, independent of optic neuritis.

Unrestricted grant from OPTOS PLC that supported the study, including the PhD studentship for G.M.

HUMAN SUBJECTS: BEAMS is a single-centre, cross-sectional, case-control study approved by the UK research ethics committee (REC 18/NW/0334) and adheres to the Declaration of Helsinki. All participants gave written consent.

Author Contributions:

Research design, Data acquisition and/or research execution, Data analysis and/or interpretation, manuscript preparation: Lajos Csincsik, Tunde Peto, Imre Lengyel

Data acquisition and/or research execution, Data analysis and/or interpretation, manuscript preparation: Gemma McIlwaine, Gavin McDonnell, Stella Hughes

Research design, Data analysis and/or interpretation, manuscript preparation: Denise Fitzgerald, Adam M Dubis

Data acquisition and/or research execution, manuscript preparation: Luping Wang, Jill Moffat

Research design, Data acquisition and/or research execution, manuscript preparation: Rachel Coey

Abbreviations and Acronyms:

AO = adaptive optics; **BM** = Bruch's membrane; **GCIPL** = ganglion cell inner plexiform layer; **GEE** = Generalized Estimating Equitation; **IOP** = intraocular pressure; **MD** = mean difference; **MS** = multiple sclerosis; **MSnON** = eyes of patients with MS without a history of optic neuritis; **MSON** = eyes of patients with MS with a history of optic neuritis;

ONH = optic nerve head; **ONL** = outer nuclear layer; **PRL** = photoreceptor segments layer; **pRNFL** = peripapillary retinal nerve fiber layer; **VA** = visual acuity.

Keywords:

Multiple sclerosis, Adaptive optics ophthalmoscope, Retina, Cone, OCT.

Correspondence:

Imre Lengyel, PhD, Wellcome-Wolfson Institute for Experimental Medicine, Queen's University, Belfast, 97 Lisburn Road, Belfast, Northern Ireland BT9 7BL, UK. E-mail: i.lengyel@qub.ac.uk.

References

- Saidha S, Al-Louzi O, Ratchford JN, et al. Optical coherence tomography reflects brain atrophy in multiple sclerosis: a four-year study. *Ann Neurol*. 2015;78:801–813.
- Balcer LJ, Miller DH, Reingold SC, Cohen JA. Vision and vision-related outcome measures in multiple sclerosis. *Brain*. 2015;138:11–27.
- Hanson JVM, Hediger M, Manogaran P, et al. Outer retinal dysfunction in the absence of structural abnormalities in multiple sclerosis. *Invest Ophthalmol Vis Sci*. 2018;59:549–560.
- Hanson JVM, Ng MY, Hayward-Koennecke HK, et al. A three-year longitudinal study of retinal function and structure in patients with multiple sclerosis. *Doc Ophthalmol*. 2022;144:3–16.
- Paul F, Calabresi PA, Barkhof F, et al. Optical coherence tomography in multiple sclerosis: a 3-year prospective multicenter study. *Ann Clin Transl Neurol*. 2021;8:2235–2251.
- Saidha S, Syc SB, Durbin MK, et al. Visual dysfunction in multiple sclerosis correlates better with optical coherence tomography derived estimates of macular ganglion cell layer thickness than peripapillary retinal nerve fiber layer thickness. *Mult Scler*. 2011;17:1449–1463.
- Fisher JB, Jacobs DA, Markowitz CE, et al. Relation of visual function to retinal nerve fiber layer thickness in multiple sclerosis. *Ophthalmology*. 2006;113:324–332.
- Gomaa S, Badawy M, Elfatry A, Elhennawy A. Visual dysfunction and neurological disability in multiple sclerosis patients in correlation with the retinal nerve fiber layer and the ganglion cell layer using optical coherence tomography. Original Article. *Egypt J Neurol Psychiatry Neurosurg*. 2016;53:200–205.
- Polman CH, Reingold SC, Banwell B, et al. Diagnostic criteria for multiple sclerosis: 2010 revisions to the McDonald criteria. *Ann Neurol*. 2011;69:292–302.
- Aytulun A, Cruz-Herranz A, Aktas O, et al. APOSTEL 2.0 recommendations for reporting quantitative optical coherence tomography studies. *Neurology*. 2021;97:68–79.
- Schneider CA, Rasband WS, Eliceiri KW. NIH Image to ImageJ: 25 years of image analysis. *Nat Methods*. 2012;9:671–675.
- Thevenaz P, Unser M. User-friendly semiautomated assembly of accurate image mosaics in microscopy. *Microsc Res Tech*. 2007;70:135–146.
- GNU Image Manipulation Program (GIMP). Version 2.10.32; 1996.* . Accessed July 6, 2022.
- Feng S, Gale MJ, Fay JD, et al. Assessment of different sampling methods for measuring and representing macular cone density using flood-illuminated adaptive optics. *Invest Ophthalmol Vis Sci*. 2015;56:5751.
- Balcer LJ, Frohman EM. Evaluating loss of visual function in multiple sclerosis as measured by low-contrast letter acuity. *Neurology*. 2010;74 Suppl 3:S16–S23.
- Murphy OC, Kalaitzidis G, Vasileiou E, et al. Optical coherence tomography and optical coherence tomography angiography findings after optic neuritis in multiple sclerosis. *Front Neurol*. 2020;11:618879.
- Frohman EM, Dwyer MG, Frohman T, et al. Relationship of optic nerve and brain conventional and non-conventional MRI measures and retinal nerve fiber layer thickness, as assessed by OCT and GDx: a pilot study. *J Neurol Sci*. 2009;282:96–105.
- Ortiz-Perez S, Martinez-Lapiscina EH, Gabilondo I, et al. Retinal periphlebitis is associated with multiple sclerosis severity. *Neurology*. 2013;81:877–881.
- Biousse V, Trichet C, Bloch-Michel E, Roullet E. Multiple sclerosis associated with uveitis in two large clinic-based series. *Neurology*. 1999;52:179–181.
- Walter SD, Ishikawa H, Galetta KM, et al. Ganglion cell loss in relation to visual disability in multiple sclerosis. *Ophthalmology*. 2012;119:1250–1257.
- Syc SB, Saidha S, Newsome SD, et al. Optical coherence tomography segmentation reveals ganglion cell layer pathology after optic neuritis. *Brain*. 2012;135(Pt 2):521–533.
- Birkeldh U, Manouchehrinia A, Hietala MA, et al. The temporal retinal nerve fiber layer thickness is the most important optical coherence tomography estimate in multiple sclerosis. *Front Neurol*. 2017;8:675.
- Sabaner MC, Duman R, Duman R, et al. Inner retinal layer disease: multiple sclerosis. *Beyoglu Eye J*. 2020;5:93–101.
- Fard MA, Golizadeh A, Yadegari S, et al. Photoreceptor outer nuclear layer thickness changes in optic neuritis follow up. *Mult Scler Relat Disord*. 2019;39:101905.
- Roshandel D, Heath Jeffery RC, Charng J, et al. Short-term parafoveal cone loss despite preserved ellipsoid zone in rod cone dystrophy. *Transl Vis Sci Technol*. 2021;10:11.
- Grimm C, Wenzel A, Hafezi F, et al. Protection of Rpe65-deficient mice identifies rhodopsin as a mediator of light-induced retinal degeneration. *Nat Genet*. 2000;25:63–66.
- Li KY, Tiruveedhula P, Roorda A. Intersubject variability of foveal cone photoreceptor density in relation to eye length. *Invest Ophthalmol Vis Sci*. 2010;51:6858.